THE JOURNAL OF PHYSICAL CHEMISTRY C

pubs.acs.org/JPCC

Article

Hydrogenation on Palladium Nanoparticles Supported by Graphene Nanoplatelets

Published as part of The Journal of Physical Chemistry virtual special issue "Metal Clusters, Nanoparticles, and the Physical Chemistry of Catalysis".

Klaus Dobrezberger, Johannes Bosters, Nico Moser, Nevzat Yigit, Andreas Nagl, Karin Föttinger, David Lennon, and Günther Rupprechter*

Cite This: *J. Phys. Chem. C* 2020, 124, 23674−23682

Read Online

ACCESS | Metrics & More | Article Recommendations

ABSTRACT: Pd nanoparticles (1 wt %; mean size ∼4 nm) were supported on ∼2 μm sized, but few nanometers thick, graphene nanoplatelets (GNPs) and compared to 1 wt % Pd on activated carbon or γ-alumina. Catalyst morphology, specific surface area, and Pd particle size were characterized by SEM, BET, and TEM, respectively. H_2-TPD indicated that GNPs intercalated hydrogen, which may provide additional H_2 supply to the Pd nanoparticles during C_2H_4 hydrogenation. Whereas the two types of Pd/GNPs (NaOH vs calcinated) catalysts were less active than Pd/C and Pd/Al_2O_3 below 40 °C, at 55 °C they were about 3−4 times more active. As for example Pd/GNPs (NaOH) and Pd/Al_2O_3 exhibited not too different mean Pd particle size (3.7 vs 2.5 nm, respectively), the higher activity is attributed to the additional hydrogen supply likely by the metal/support interface, as suggested by the varying C_2H_4 and H_2 orders on the different supports. *Operando* XANES measurements during C_2H_4 hydrogenation revealed the presence of Pd hydride. The Pd hydride was more stable for Pd/GNPs (NaOH) than for Pd/C, once more pointing to a better hydrogen supply by graphene nanoplatelets.

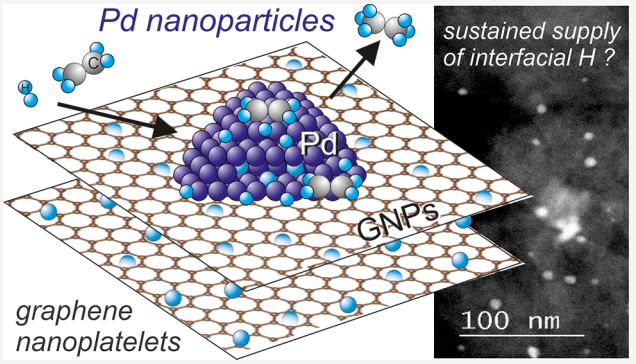

1. INTRODUCTION

Supported Pd catalysts are particularly important for industrial hydrogenation reactions, including fine chemicals synthesis.[1−3] Palladium is considered the most selective among the platinum metals, as hydrogenation is much faster than dehydrogenation to undesired carbonaceous species. High dispersion (mean Pd particle sizes below 3 nm) is a prime asset of these catalysts. Clearly, the nature of the support has a strong influence on performance, with carbon-based materials, alumina, and silica being most frequently applied. Resulting from their practical importance, technological as well as model catalysts of Pd/Al_2O_3, Pd/Fe_3O_4, or Pd/C (activated carbon, nanotubes, planar graphene layers, highly oriented pyrolytic graphite (HOPG), etc.) have been repeatedly studied for the (selective) hydrogenation of for example ethylene,[4−9] 1,3-butadiene,[10−13] 1-butene,[14] acetylene,[5,15] 1-propyne,[16,17] unsaturated aldehydes,[18] and others.[4,19−21] For reviews and more detailed accounts we refer to refs 21−33.

When carbon was used as catalyst support, many different types and morphologies have been examined,[1] including activated carbon, carbon black, graphite, and various forms of graphene (GN), such as (single and multiwalled) nanotubes, (exfoliated) sheets, nanoplatelets (GNP), etc. Graphene-supported Pt nanoparticles have received particular attention because of their use in polymer electrolyte membrane (PEM) fuel cells (hydrogen or methanol oxidation). They were reported to exhibit higher electrocatalytic activity, stability, and poisoning tolerance than Pt/activated carbon, which also enabled to reduce the Pt loading.[34−36] For graphene-supported Pd there are fewer studies, but similarly, electrocatalytic oxidation and hydrogenation activity were higher than for traditional carbon supports.[37−39] Carbon and Pd/GN(P) received further attention for hydrogen storage, again relevant for fuel cell technology.[40−42]

In this contribution, we have exploited graphene nanoplatelets (GNPs) as support for Pd nanoparticles and contrasted them to Pd/activated carbon and Pd/Al_2O_3.

Received: July 20, 2020
Revised: October 6, 2020
Published: October 19, 2020

https://dx.doi.org/10.1021/acs.jpcc.0c06636
J. Phys. Chem. C 2020, 124, 23674−23682

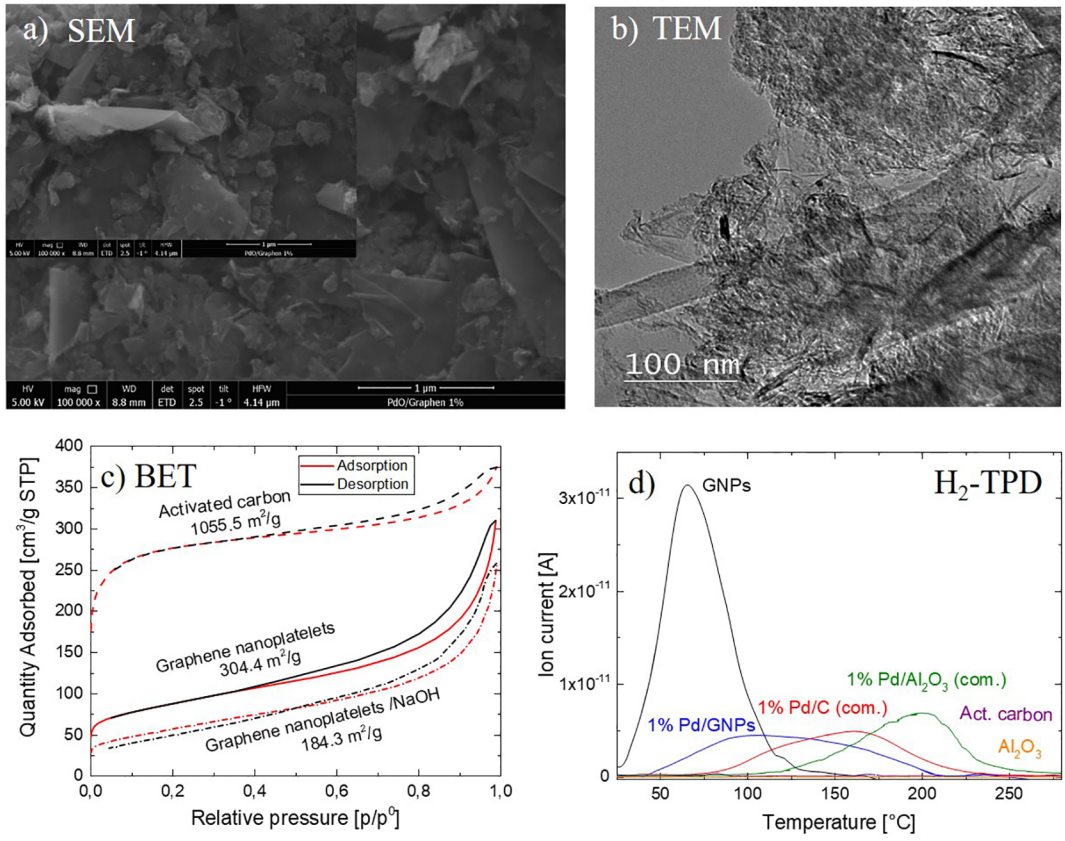

Figure 1. Characterization of graphene nanoplatelets (GNPs): (a) SEM and (b) TEM images. (c) N_2 physisorption (adsorption/desorption) (with/without basic treatment; activated carbon included for comparison). (d) H_2-TPD (contrasted to activated carbon, Pd/GNPs, Pd/C, Pd/Al_2O_3, and Al_2O_3; H_2 exposed at room temperature, evacuated; heating ramp 10 °C/min).

Ethylene hydrogenation, following Langmuir−Hinshelwood kinetics via stepwise hydrogenation (a mechanism proposed by Horiuti and Polanyi in 1934), is a prototype test reaction providing valuable information about catalytic performance, reaction mechanisms, and deactivation processes.[5]

$$C_2H_4 + H_2 \rightarrow C_2H_6 \quad \Delta H_{298\,K} = -137\ \text{kJ/mol}$$

Although this reaction does not hold selectivity issues (if one neglects C_2H_4 decomposition), it has still proven very useful to examine C_2H_4 adsorption, C_2H_4/H coadsorption, and the effects of subsurface hydrogen and Pd hydride formation, altogether suggesting the addition of hydrogen to an adsorbed π-bonded ethylene being rate limiting.[4−9,43,44]

For reaction temperatures above 40 °C, higher activities (turnover frequencies TOFs) were observed for Pd nanoparticles supported by GNPs, which may be related to hydrogen storage/intercalation by the graphene nanoplatelets. *Operando* studies under reaction conditions were performed by X-ray absorption near-edge structure (XANES) spectroscopy, revealing Pd hydride. The higher activity was attributed to the additional hydrogen supply, as corroborated by the varying C_2H_4 and H_2 orders on the different supports. Clearly, more detailed (preferentially *operando*) studies are required, but the current results already indicate the high potential of Pd supported on graphene nanoplatelets as a hydrogenation catalyst.

2. METHODS

2.1. Materials and Catalyst Preparation. Graphene nanoplatelets (GNPs) and palladium acetate as metal precursor[45] (both from Sigma-Aldrich) were used for two types of synthesis: (i) wet impregnation with formaldehyde as reducing agent[46] in basic medium (NaOH; pH 12)[47] and (ii) wet impregnation followed by calcination in air.

For wet impregnation (i), specific amounts of GNPs and precursor (Pd^{2+} ac) were suspended in 50 mL of water (with a small amount of ethanol for better dispersion) and stirred at room temperature for 30 min, after which formaldehyde was added as reducing agent. Sodium hydroxide (pH 12) was added, as it was reported to improve particle nucleation. Finally, the precatalyst was obtained by filtration and drying at 100 °C for 3 h (Pd/GNPs (NaOH)).

For wet impregnation (ii), the support and precursor mixture were stirred in toluene at 60 °C, filtered, dried at 100 °C (3 h), and calcinated at 300 °C in air (Pd/GNPs (calc)).

For comparison and benchmarking, commercial 1% Pd/activated carbon and 1% Pd/γ-alumina (both from Sigma-Aldrich) were examined.[17] The activation treatment of all catalysts is described below.

2.2. Catalyst Characterization. Characterization was carried by various techniques:

SEM/EDX and TEM/HAADF-STEM: Scanning electron microscopy (SEM) was used to determine the morphology of the graphene nanoplatelets. Using energy dispersive X-ray fluorescence (EDX), we confirmed the absence of impurities.

https://dx.doi.org/10.1021/acs.jpcc.0c06636
J. Phys. Chem. C 2020, 124, 23674−23682

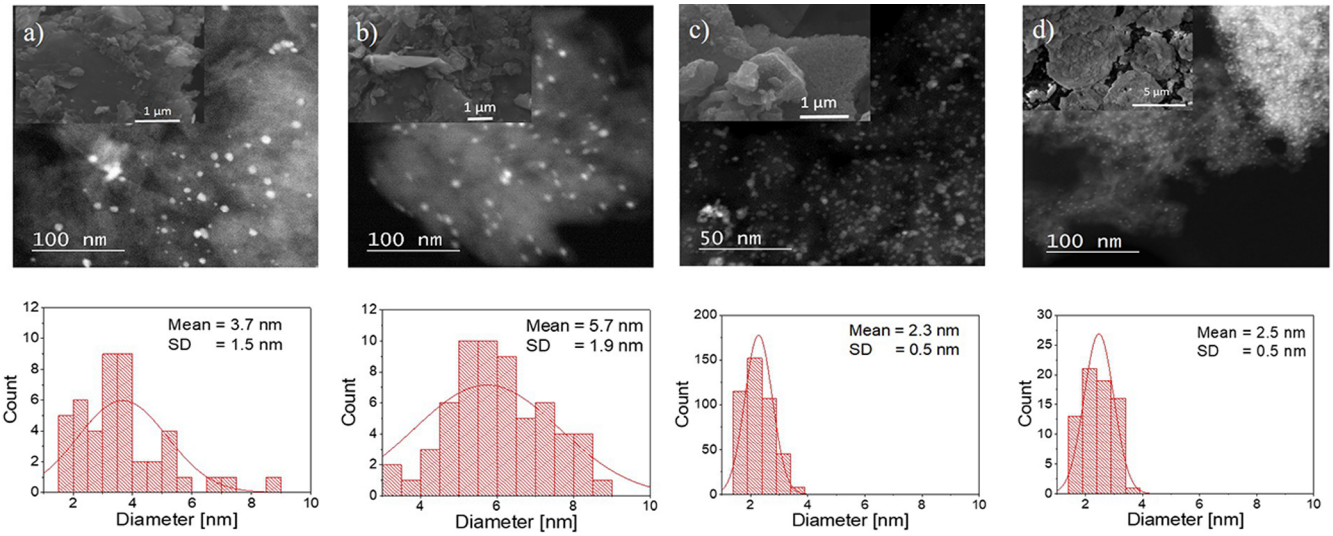

Figure 2. HAADF-STEM and SEM (inset) images and corresponding Pd particle size distributions of (a) 1% Pd/GNPs (NaOH), (b) 1% Pd/GNPs (calc), and (c) 1% Pd/C and 1% Pd/Al_2O_3.

To determine the metal nanoparticle size distribution, transmission and high angle annular dark field scanning transmission electron microscopy (TEM/HAADF-STEM) were performed (FEI-TECNAI F20; "ImageJ" software) for pretreated catalysts.

N_2 physisorption (BET): For determining the specific surface area (SSA) of the samples, N_2 physisorption was performed at −196 °C (ASAP 2020 Micromeretics).[37] Using ca. 100 mg sample, we performed degassing at 350 °C for 4 h (temperature ramp of 10 °C/min) to remove adsorbed water. Data analysis was performed by using the Brunauer−Emmett−Teller (BET) method.

CO chemisorption: As alternative measurement of the average Pd nanoparticle diameter (apart from TEM), quantitative chemisorption of CO was performed for pretreated catalysts. The particle diameter was calculated by assuming hemispherical particles, with a stoichiometric factor (per Pd surface atom) of 1 for CO. A 0.5 g sample was placed into a quartz tube for measurements at 35 °C (10−860 mbar) and analyzed as described by Canton et al.[48]

H_2-TPD: Temperature-programmed desorption (TPD) of H_2 was performed by using a 0.1 g sample of support or (pretreated) catalysts. Hydrogen (100 mbar) was dosed at room temperature for 30 min, followed by evacuation for 30 min. For TPD, a heating rate of 10 °C/min was applied.

ζ-potential: To investigate the effect of the pH value, the surface potential of the sample was determined (ζ-potential[49,50]). Palladium ions (Pd^{2+}) that were used as precursor likely interact stronger with a negatively charged support surface, created for example by adding sodium hydroxide to increase the pH to 12.[51]

X-ray absorption near-edge structure (XANES): *Operando* X-ray absorption spectroscopy (focusing on the near-edge structure) was performed in transmission mode at the ALBA-Synchrotron beamline (CLAESS, Barcelona).[52,53] XANES measurements of pellets (sample diluted 1:10 with BN) were compared with models of hydrogen absorption reported in refs 52 and 53.

2.3. Catalytic Reaction. For kinetic measurements of ethylene hydrogenation, a fully automated plug-flow reactor was used ("Microeffi" from PID Comp.), coupled to a micro-GC (Inficon) with two columns (PlotQ and Molsieve). Because of the high activity of supported Pd, about 5 mg of catalyst was diluted with 995 mg of SiO_2. For kinetic tests, 10 mg of the "diluted" catalyst was used. For catalyst activation (pretreatment) before the reaction, the carbon-supported catalysts (Pd/GNPs (NaOH) and Pd/GNPs (calc), Pd/C) were reduced in 8% H_2 in He (total flow: 100 mL/min) at 200 °C (2 h), whereas Pd/γ-alumina was activated in 20% O_2 in He (total flow: 100 mL/min) at 500 °C (2 h), followed by reduction in 8% H_2 in He (total flow: 100 mL/min) at 200 °C (2 h).

For the ethylene hydrogenation, a mixture of 2 vol % C_2H_4 and 20 vol % H_2 in He at a total flow of 100 mL/min was used. GC measurements were taken from 25 to 55 °C, in steps of 5 °C. The reaction rate was calculated via the following equation: reaction rate [mol/(s g)] = (ethylene conversion × ethylene flow [mol/s])/(amount of catalyst (without SiO_2) [g]). Additionally, rates were normalized per gram of Pd or per Pd surface atom (turnover frequency, TOF). Reaction orders were determined at 55 °C for C_2H_4 (from 1 to 8 vol % C_2H_4 in 0.5 vol % steps at constant 20 vol % H_2) and H_2 (from 3 to 18 vol % in 3 vol % steps at constant 2 vol % C_2H_4).

3. RESULTS AND DISCUSSION

3.1. Graphene Nanoplatelets (GNPs). SEM and TEM images of the graphene nanoplatelets (GNPs) are shown in Figures 1a and 1b, respectively. The GNPs were typically less than 2 μm in diameter and a few nanaometers in thickness but often seem thicker due to stacking/aggregation. EDX detected only C, Na, and O but no (metal) impurities. Because of nonoxidizing manufacturing, the GNPs have a pristine graphitic surface with sp^2 carbon. N_2 physisorption (Figure 1c) indicated a SSA of 304 and 184 m^2/g without and with NaOH treatment, respectively (activated carbon is included for comparison). The effect of NaOH treatment will be discussed below. H_2-TPD from GNPs is contrasted to activated carbon in Figure 1d. The graphene nanoplatelets "stored" significant amounts of hydrogen, likely by intercalation between the nanosheets (macroporosity), which then desorbed above 50 °C. Activated carbon (and Al_2O_3) did not show this effect.

https://dx.doi.org/10.1021/acs.jpcc.0c06636
J. Phys. Chem. C 2020, 124, 23674−23682

Table 1. Summary of Characterization Results: BET Surface, Mean Pd Particle Diameter, and Dispersion via TEM and CO Chemisorption

		BET	TEM		CO chemisorption	
catalyst	nominal metal loading [wt %]	surface area [m^2/g]	mean Pd diameter [nm]	Pd dispersion [%]	mean Pd diameter [nm]	Pd dispersion [%]
GNPs	0	304.4				
activated carbon	0	1055.5				
Pd/GNPs (NaOH)	1	184.3	3.7	38.3	3.8	37.5
Pd/GNPs (calc)	1	278.2	5.7	26.3	5.9	25.5
Pd/C (com)	1	959.0	2.3	56.0	1.6	71.7
Pd/Al_2O_3 (com)	1	200.6	2.5	52.6	2.2	57.8

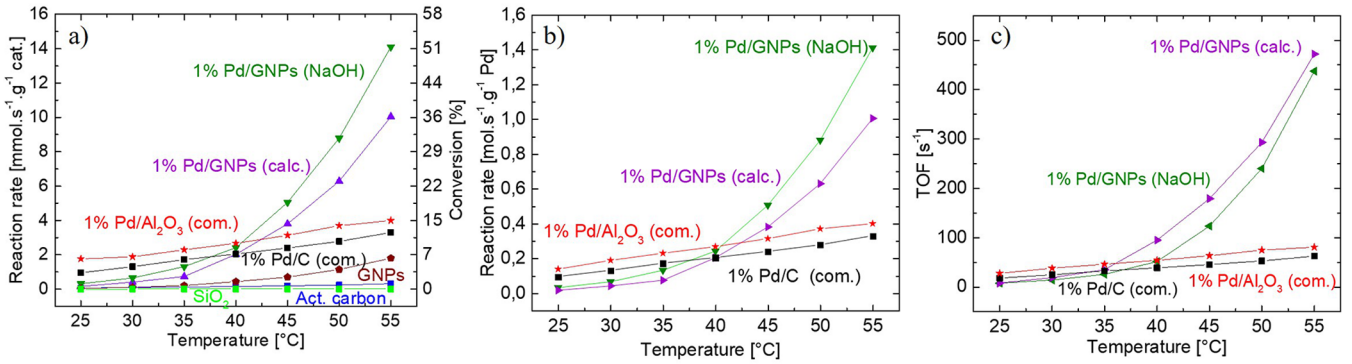

Figure 3. C_2H_4 hydrogenation at various reaction temperatures for 1% Pd/GNPs (NaOH), 1% Pd/GNPs (calc), and 1% Pd/C and 1% Pd/Al_2O_3: (a) reaction rates per gram of catalyst, not accounting for SiO_2 dilution, (b) reaction rates per gram of Pd, and (c) turnover frequencies (TOF). Conversion is included in (a).

Table 2. Summary of Kinetic Results[a]

catalyst	metal loading [%]	rate at 30 °C [mol s^{-1} g^{-1}] (sample or Pd)	rate at 55 °C [mol s^{-1} g^{-1}] (sample or Pd)	E_a [kJ/mol]	C_2H_4 order	H_2 order
GNPs	0	1.0×10^{-4}	1.8×10^{-3}	109.5	0.06	0.72
activated carbon	0	1.1×10^{-5}	1.1×10^{-3}	98.1	0.03	0.66
Pd/GNPs (NaOH)	1	0.07	1.41	106.2	0.21	0.77
Pd/GNPs (calc)	1	0.05	1.01	115.0	0.35	0.75
Pd/C (com)	1	0.13	0.33	32.4	−0.20	0.90
Pd/Al_2O_3 (com)	1	0.19	0.40	28.3	−0.05	0.95

[a]The reaction rate was determined at 30 and 55 °C; reaction orders were measured at 55 °C.

3.2. Pd Nanoparticles Supported by Graphene Nanoplatelets (Pd/GNPs). As described in section 2.2, the GNPs were used as support for Pd nanoparticles, employing different synthesis protocols. Figure 2 shows HAADF-STEM and SEM images, as well as the corresponding Pd particle size distributions, for 1% Pd/GNPs (NaOH), 1% Pd/GNPs (calc.), and commercial 1% Pd/C and 1% Pd/Al_2O_3. All structural parameters, including results from BET and chemisorption, are summarized in Table 1. H_2-TPD from (pretreated) Pd/GNPs in Figure 1d showed desorption over a broad temperature range, apparently with contributions from both GNPs and Pd nanoparticles (cf. Pd/C and Pd/Al_2O_3).

As mentioned, route i was impregnation with reduction by formaldehyde in basic (NaOH) medium. BET indicated that NaOH reduced the SSA (from 304 to 184 m^2/g) but increased the ζ-potential of GNPs (−3.3 mV at pH = 7 to −17.4 mV at pH = 12). Consequently, Pd^{2+} ions of the precursor interacted stronger with the negatively charged GNPs surface, creating higher Pd dispersion (~38%) with a mean Pd particle size of 3.7 nm (with TEM and chemisorption agreeing well; Table 1). Furthermore, NaOH may also create surface defects acting as nucleation centers.[54]

Route ii included impregnation, calcination in air at 300 °C, and H_2 reduction at 200 °C. This maintained a higher SSA (278 m^2/g), but the Pd nanoparticles were larger (mean size 5.7 nm; ~26% dispersion), again with TEM in agreement with chemisorption (Table 1). Apparently, calcination at 300 °C already induces Pd particle sintering on GNPs.

Commercial 1% Pd/C had a mean Pd particle size of 2.3 nm (dispersion ~56%), similar to commercial Pd/Al_2O_3 (mean Pd particle size of 2.5 nm, dispersion ~53%). For the smaller particle sizes, TEM and chemisorption somewhat deviated, which has been repeatedly reported.[55,56] TEM may "overlook" the smallest sizes, and some of the assumptions of chemisorption analysis (specific adsorption on the metal, fixed CO:Pd adsorption ratio and geometry) may no longer be valid.

3.3. Kinetics of C_2H_4 Hydrogenation on Pd/GNPs. The Pd nanoparticles (1 wt %) on different supports were tested for ethylene hydrogenation. Minor deactivation (approximately 1−5% of total conversion, depending on reaction temperature)

https://dx.doi.org/10.1021/acs.jpcc.0c06636
J. Phys. Chem. C 2020, 124, 23674−23682

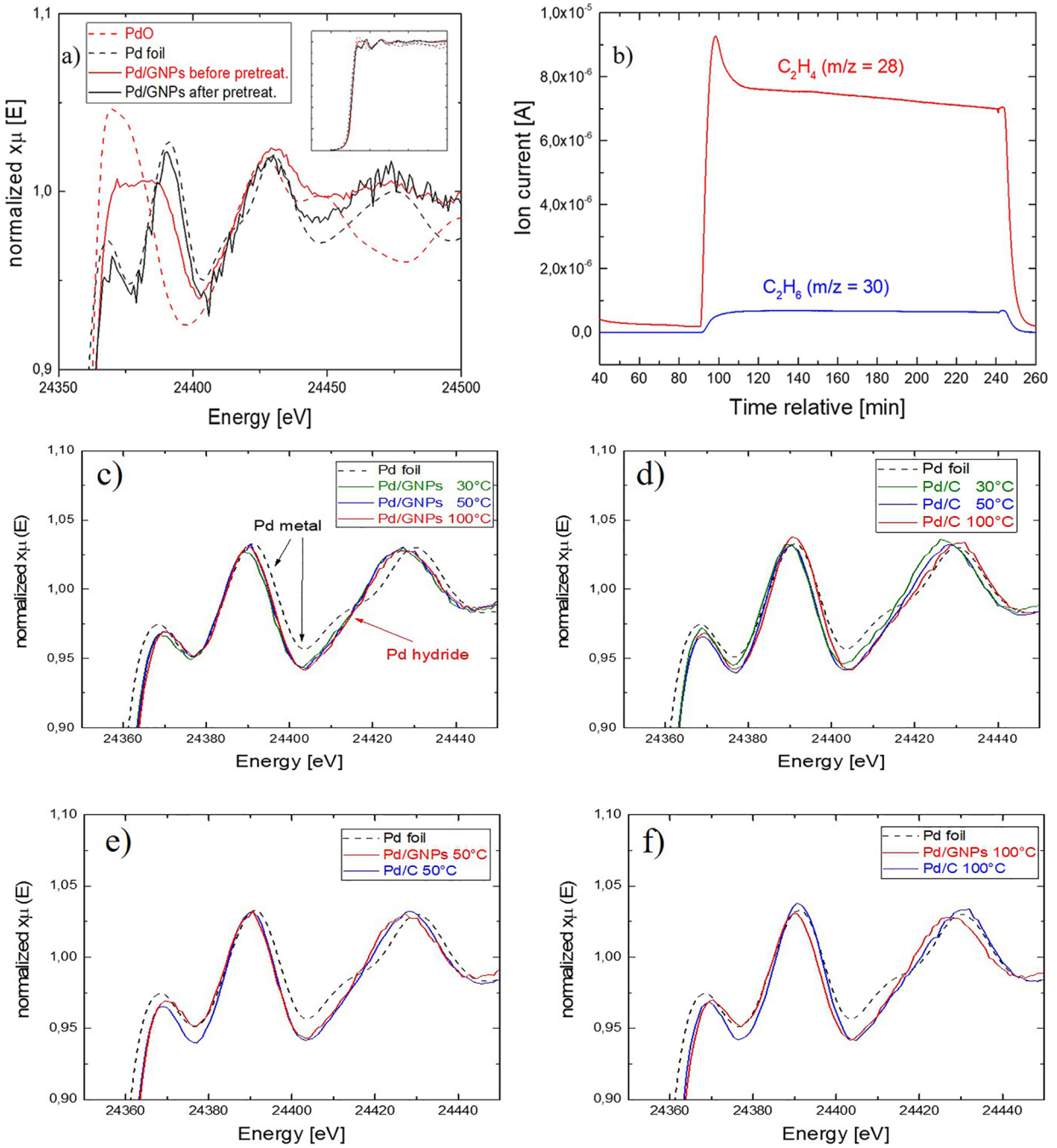

Figure 4. *In situ* XANES measurements of (a) 1% Pd/GNPs (NaOH), before and after pretreatment (H_2 200 C, cooldown in He) (Pd foil and PdO in vacuum are included as reference). (b) Mass spectroscopy (MS) traces under reaction conditions, simultaneously measured with (c–f) *operando* XANES during C_2H_4 hydrogenation on (c) Pd/GNPs (NaOH) and (d) Pd/C (Pd foil in a vacuum is included as reference). (e, f) Direct comparison of Pd/GNPs and Pd/C under reaction conditions with temperatures indicated.

occurred in the first 20 min, likely due to carbon deposition, so that steady-state data after 40 min reaction time are reported herein. The results are summarized in Figure 3 and Table 2. Reaction rates are normalized to the catalyst weight (ignoring the dilution by inert SiO_2) per gram of Pd and per Pd surface atom. Conversions ranged from 0.5 to 51%.

Activated carbon exhibited no activity at all, whereas pure graphene nanoplatelets had low activity at 55 °C (alkene hydrogenation on GNPs at 110 °C has been reported in Primo et al.[57]). As mentioned, EDX analysis of GNPs indicated no metal impurities, but it cannot be excluded that metal traces were responsible for the small activity.

Below 40 °C, the Pd nanoparticles supported on GNPs (for both preparation routes) were less active than Pd/C or Pd/Al_2O_3. Above 40 °C, the activities reversed, with Pd/GNPs being ~3–4 times more active than Pd/C or Pd/Al_2O_3. This behavior led to apparently much higher activation energies on Pd/GNPs (Table 2). Comparing the E_a values for the GNP-supported Pd against that of Pd/Al_2O_3 and Pd/C indicates differences in the surface chemistry when GNP are used to support Pd crystallites. This outcome suggests different metal/

https://dx.doi.org/10.1021/acs.jpcc.0c06636
J. Phys. Chem. C 2020, 124, 23674–23682

support interactions are active with the Pd/GNP catalyst. The origin of the higher activity of Pd/GNPs may be related to the larger Pd particle size (~4 nm vs ~2 nm; with smaller particles being more easily deactivated) and/or the nature of the support (GNPs vs C or Al_2O_3). Also, sodium seems to have a beneficial effect (cf. Pd/GNPs(NaOH) vs Pd/GNPs(calc)), which may be due to higher dispersion. Indeed, with respect to turnover frequencies (Figure 3c), the two GNPs-supported catalysts reversed, and 1% Pd/GNPs (calc) was the most active.

To further investigate differences between the catalysts, the C_2H_4 and H_2 reaction orders were determined at 55 °C (Table 2). For Pd/C and Pd/Al_2O_3, the C_2H_4 orders are (slightly) negative (in agreement with model studies; −0.3 in ref 58), which indicates that under these conditions ethylene already blocks the Pd surface. In contrast, for Pd/GNPs the C_2H_4 order is clearly positive, which indicates that the Pd surface was not yet saturated with C_2H_4. Concerning H_2 order, it is ~1 for Pd/C and Pd/Al_2O_3 but ~0.75 for Pd/GNPs. This also confirms that the Pd surface of Pd/GNPs is more readily available for the reactants. For Pd single crystal and Pd/Al_2O_3, C_2H_4 and H_2 reaction orders of approximately 0 and 1 were reported in the literature,[59,60] respectively.[61]

Several effects may account for these observations. Most importantly, the GR nanoplatelets intercalated hydrogen and released it around 40 °C (note that this is the temperature of the activity reversal), which creates additional hydrogen supply to a Pd particle, in addition to the gas phase route (a similar effect was reported by Rupprechter and Somorjai[62]). Although the GNPs supported Pd particles are a bit larger, one cannot exclude electronic metal−support interactions (especially at the phase boundary). Indeed, graphene has been shown to be an excellent support for CuZn nanoparticles for methanol synthesis.[63] Last but not least, the smaller Pd nanoparticles on activated carbon or alumina may be more prone to partial deactivation by carbonaceous species (CH_x), as reported by Lennon and co-workers.[17]

3.4. *Operando* Studies of C_2H_4 Hydrogenation on Pd/GNPs. Figure 4a shows *in situ* XANES spectra of (the smaller) Pd nanoparticles on GNPs (NaOH), before and after H_2 pretreatment (without intermittent exposure to the atmosphere). Pd foil and PdO were measured in a vacuum as reference. Before H_2 pretreatment, the Pd particles were partially oxidized but metallic after reduction (with cooldown in He to avoid Pd hydride formation).[6,62]

C_2H_4 hydrogenation was then performed under the mentioned reaction conditions at 30, 50, and 100 °C, with the gas composition monitored by mass spectroscopy (MS), shown in Figure 4b. *Operando* XANES spectra of Pd/GNPs (NaOH) and Pd/C are displayed in Figures 4c and 4d, respectively (Pd foil is again added just as reference; i.e., it is not measured under reaction conditions). Apparently, both Pd/GNPs and Pd/C showed the presence of Pd hydride in the entire temperature range (reaction flow conditions equivalent to 200 mbar of H_2). Thermal desorption spectroscopy (TDS) of model catalysts had suggested a strongly enhanced hydrogenation probability in the presence of Pd hydrides, for both Pd nanoparticles and Pd single crystals (the conversion of C_2H_4 being nearly 100% in the presence of palladium hydrides).[4,6,43] For Pd/C, the hydride phase seems more pronounced at lower temperature (30 °C) than at higher temperature (100 °C), pointing to hydride decomposition, which may be facilitated for smaller particles.

A direct comparison of Pd/GNPs and Pd/C at 50 and 100 °C (Figure 4e,f) reveals almost identical spectra at 50 °C, but at 100 °C the hydride is still present for Pd/GNPs but seems (more) decomposed for Pd/C. This indicates a Pd particle size and/or support effect (with larger particles and GNPs supplying more hydrogen to the Pd particles).

Parker, Albers, and co-workers have used the technique of inelastic neutron scattering (INS) to investigate the matter of hydride formation in supported Pd catalysts. Application of carbon-supported Pd catalysts for the hydrogenation of nitroarenes showed that carbon exhibiting enhanced sp^2 character templated the binding of the Pd particles at the edges of carbon particles. Catalytic activity was attributed to (i) hydrogen storage capability and (ii) the availability of that reservoir of hydrogen.[64] Follow-on work established the influence of the support material, which critically can affect the rate of release of stored hydrogen from the Pd particles.[65] Thus, in addition to verifying a role for Pd hydride in heterogeneously catalyzed hydrogenation reactions, the INS studies also reveal how important the nature and form of the metal/support interface are in affecting hydrogen supply for subsequent reaction at the Pd surface.

Given that Figure 4 shows the extent of Pd hydride in the Pd/GNPs and Pd/C samples to be broadly comparable, this indicates that it is not simply the presence or absence of a hydride phase that is affecting the favorable hydrogenation performance of Pd/GNPs compared to Pd/C as evidenced in Figure 3. However, with reference to the aforementioned INS studies, this apparent discrepancy hints at a discrete role for hydrogen at the metal/support interface and the relative availability of that hydrogen for reaction. Chesters and co-workers used ^1H NMR spectroscopy to examine hydrogen chemisorption over a silica-supported Pt catalyst and report the presence of a resonance that is assigned to hydrogen present at the interface between the Pt particles and the support material.[66] Further variable temperature NMR studies concentrating on the EuroPt-1 reference catalyst endorse the generality of the models proposed and provide insight into the dynamics of hydrogen chemisorbed over supported metal particles.[67]

Linking these strands together, the origin of the enhanced hydrogenation performance observed for the Pd/GNP (Figure 3) is thought to be that the graphene nanoplatelets foster binding to the Pd crystallites that can additionally accommodate hydrogen atom transfer at the metal/support interface. Then, warming the catalyst above 40 °C increases the mobility of this interfacial hydrogen such that it becomes available for reaction. Thus, although possessing a comparable Pd particle size to that of Pd/C (section 3.2), it is the nature of the graphene nanoplatelets of the Pd/GNPs that *facilitates hydrogen availability at the metal/support interface*. The ethene hydrogenation reaction profiles presented in Figure 3 indicate that the activated carbon used for the Pd/C catalyst cannot similarly buffer surface the hydrogen supply in this way.

4. CONCLUSIONS

Pd nanoparticles, with mean sizes around 4 and 2 nm, were supported on either graphene nanoplatelets (GNPs), activated carbon, or γ-alumina. Apart from apparent differences in specific surface area (SSA), H_2-TPD indicated that GNPs intercalated hydrogen which may provide an additional supply of hydrogen to the Pd nanoparticles (apart from the direct adsorption from the gas phase). For ethylene hydrogenation,

https://dx.doi.org/10.1021/acs.jpcc.0c06636
J. Phys. Chem. C 2020, 124, 23674−23682

Pd/GNPs (NaOH and calc) were less active than Pd/C and Pd/Al_2O_3 below 40 °C, but at 55 °C they were about 3−4 times more active. As Pd/GNPs (NaOH) and Pd/Al_2O_3 exhibited not too different mean Pd particle size (3.7 vs 2.5 nm, respectively), this effect seems related to the additional hydrogen supply (likely at the metal/support interface), as corroborated by the measured C_2H_4 and H_2 orders of the reaction. *Operando* XANES measurements during ethylene hydrogenation revealed the presence of Pd hydride. However, the Pd hydride was more stable for Pd/GNPs (NaOH) than for Pd/C, once more pointing to a better hydrogen supply by graphene nanoplatelets. Pd/GNPs will be employed for further reaction studies in the near future. Moreover, given the emphasis of temperature-dependent interfacial effects revealed here, that work will include theoretical studies (density functional theory) alongside experimental testing.

AUTHOR INFORMATION

Corresponding Author

Günther Rupprechter − *Institute of Materials Chemistry, Technische Universität Wien, 1060 Wien, Austria;* orcid.org/0000-0002-8040-1677; Email: guenther.rupprechter@tuwien.ac.at

Authors

Klaus Dobrezberger − *Institute of Materials Chemistry, Technische Universität Wien, 1060 Wien, Austria*

Johannes Bosters − *Institute of Materials Chemistry, Technische Universität Wien, 1060 Wien, Austria*

Nico Moser − *Institute of Materials Chemistry, Technische Universität Wien, 1060 Wien, Austria*

Nevzat Yigit − *Institute of Materials Chemistry, Technische Universität Wien, 1060 Wien, Austria*

Andreas Nagl − *Institute of Materials Chemistry, Technische Universität Wien, 1060 Wien, Austria*

Karin Föttinger − *Institute of Materials Chemistry, Technische Universität Wien, 1060 Wien, Austria;* orcid.org/0000-0002-2193-0755

David Lennon − *School of Chemistry, University of Glasgow, Glasgow G12 8QQ, Scotland, U.K.;* orcid.org/0000-0001-8397-0528

Complete contact information is available at: https://pubs.acs.org/10.1021/acs.jpcc.0c06636

Notes

The authors declare no competing financial interest.

ACKNOWLEDGMENTS

G.R. acknowledges the Austrian Science Fund (FWF) for support via projects (Single Atom Catalysis (I 4434-N) and DK+ Solids4Fun (W1243). XANES experiments were performed at the CLÆSS beamline at ALBA Synchrotron under CALIPSOplus funding (Grant 730872). Help in sample characterization by Michael Stöger-Pollach, Stefan Löffler, Maximilian Palir, Gerd Mauschitz (all TU Wien), and ALBA staff is appreciated.

REFERENCES

(1) Auer, E.; Freund, A.; Pietsch, J.; Tacke, T. Carbons as Supports for Industrial Precious Metal Catalysts. *Appl. Catal., A* **1998**, *173* (2), 259−271.

(2) McAllister, M. I.; Boulho, C.; McMillan, L.; Gilpin, L. F.; Wiedbrauk, S.; Brennan, C.; Lennon, D. The Production of Tyramine: Via the Selective Hydrogenation of 4-Hydroxybenzyl Cyanide over a Carbon-Supported Palladium Catalyst. *RSC Adv.* **2018**, *8* (51), 29392−29399.

(3) McAllister, M. I.; Boulho, C.; Brennan, C.; Parker, S. F.; Lennon, D. Toward Sustained Product Formation in the Liquid-Phase Hydrogenation of Mandelonitrile over a Pd/C Catalyst. *Org. Process Res. Dev.* **2020**, *24* (6), 1112−1123.

(4) Doyle, A. M.; Shaikhutdinov, S. K.; Jackson, S. D.; Freund, H.-J. Hydrogenation on Metal Surfaces: Why Are Nanoparticles More Active than Single Crystals? *Angew. Chem., Int. Ed.* **2003**, *42*, 5240−5243.

(5) Bos, A. N. R.; Botsma, E. S.; Foeth, F.; Sleyster, H. W. J.; Westerterp, K. R. A Kinetic Study of the Hydrogenation of Ethyne and Ethene on a Commercial Pd/Al_2O_3 Catalyst. *Chem. Eng. Process.* **1993**, *32* (1), 53−63.

(6) Morkel, M.; Rupprechter, G.; Freund, H.-J. Finite Size Effects on Supported Pd Nanoparticles: Interaction of Hydrogen with CO and C_2H_4. *Surf. Sci.* **2005**, *588* (1−3), 209−219.

(7) Freund, H.-J.; Bäumer, M.; Libuda, J.; Risse, T.; Rupprechter, G.; Shaikhutdinov, S. Preparation and Characterization of Model Catalysts: From Ultrahigh Vacuum to in Situ Conditions at the Atomic Dimension. *J. Catal.* **2003**, *216* (1−2), 223−235.

(8) Zaera, F.; Somorjai, G. A. Hydrogenation of Ethylene over Platinum (111) Single-Crystal Surfaces. *J. Am. Chem. Soc.* **1984**, *106* (8), 2288−2293.

(9) Stacchiola, D.; Azad, S.; Burkholder, L.; Tysoe, W. T. An Investigation of the Reaction Pathway for Ethylene Hydrogenations on Pd(111). *J. Phys. Chem. B* **2001**, *105* (45), 11233−11239.

(10) Silvestre-Albero, J.; Rupprechter, G.; Freund, H.-J. From Pd Nanoparticles to Single Crystals: 1,3-Butadiene Hydrogenation on Well-Defined Model Catalysts. *Chem. Commun.* **2006**, No. 1, 80−82.

(11) Tardy, B.; Noupa, C.; Leclercq, C.; Bertolini, J. C.; Hoareau, A.; Treilleux, M.; Faure, J. P.; Nihoul, G. Catalytic Hydrogenation of 1,3-Butadiene on Pd Particles Evaporated on Carbonaceous Supports: Particle Size Effect. *J. Catal.* **1991**, *129* (1), 1−11.

(12) Constant, L.; Ruiz, P.; Abel, M.; Robach, P.; Porte, L.; Bertolini, J. C. Pd Deposited on Cu(110): A Highly Performant Catalyst for the 1,3-Butadiene Hydrogenation Reaction. *Top. Catal.* **2000**, *14*, 125−129.

(13) Yan, H.; Cheng, H.; Yi, H.; Lin, Y.; Yao, T.; Wang, C.; Li, J.; Wei, S.; Lu, J. Single-Atom Pd_1/Graphene Catalyst Achieved by Atomic Layer Deposition: Remarkable Performance in Selective Hydrogenation of 1,3-Butadiene. *J. Am. Chem. Soc.* **2015**, *137* (33), 10484−10487.

(14) Markova, V. K.; Philbin, J. P.; Zhao, W.; Genest, A.; Silvestre-Albero, J.; Rupprechter, G.; Rösch, N. Catalytic Transformations of 1-Butene over Palladium. A Combined Experimental and Theoretical Study. *ACS Catal.* **2018**, *8* (7), 5675−5685.

(15) Khan, N. A.; Uhl, A.; Shaikhutdinov, S.; Freund, H.-J. Alumina Supported Model Pd-Ag Catalysts: A Combined STM, XPS, TPD and IRAS Study. *Surf. Sci.* **2006**, *600* (9), 1849−1853.

(16) Lear, T.; Marshall, R.; Gibson, E. K.; Schütt, T.; Klapötke, T. M.; Rupprechter, G.; Freund, H.-J.; Winfield, J. M.; Lennon, D. A Model High Surface Area Alumina-Supported Palladium Catalyst. *Phys. Chem. Chem. Phys.* **2005**, *7* (4), 565−567.

(17) Kennedy, D. R.; Webb, G.; Jackson, S. D.; Lennon, D. Propyne Hydrogenation over Alumina-Supported Palladium and Platinum Catalysts. *Appl. Catal., A* **2004**, *259* (1), 109−120.

(18) McInroy, A. R.; Uhl, A.; Lear, T.; Klapötke, T. M.; Shaikhutdinov, S.; Schauermann, S.; Rupprechter, G.; Freund, H.-J.; Lennon, D. Morphological and Chemical Influences on Alumina-Supported Palladium Catalysts Active for the Gas Phase Hydrogenation of Crotonaldehyde. *J. Chem. Phys.* **2011**, *134* (21), 214704.

(19) Zea, H.; Lester, K.; Datye, A. K.; Rightor, E.; Gulotty, R.; Waterman, W.; Smith, M. The Influence of Pd-Ag Catalyst Restructuring on the Activation Energy for Ethylene Hydrogenation in Ethylene-Acetylene Mixtures. *Appl. Catal., A* **2005**, *282* (1−2), 237−245.

(20) Bertolini, J. C.; Delichere, P.; Khanra, B. C.; Massardier, J.; Noupa, C.; Tardy, B. Electronic Properties of Supported Pd Aggregates in Relation with Their Reactivity for 1,3-Butadiene Hydrogenation. *Catal. Lett.* **1990**, *6*, 215−223.
(21) Arnold, H.; Döbert, F.; Gaube, J. Organic Reactions: Hydrogenation Reactions: Selective Hydrogenation of Hydrocarbons. In *Handbook of Heterogeneous Catalysis*; Ertl, P. D. G., Knözinger, P. D. H., Weitkamp, P. D. J., Eds.; Wiley-VCH Verlag GmbH & Co. KGaA: Weinheim, 2008.
(22) Lan, X.; Wang, T. Highly Selective Catalysts for the Hydrogenation of Unsaturated Aldehydes: A Review. *ACS Catal.* **2020**, *10* (4), 2764−2790.
(23) Zaera, F. The Surface Chemistry of Metal-Based Hydrogenation Catalysis. *ACS Catal.* **2017**, *7* (8), 4947−4967.
(24) Aleksandrov, H. A.; Viñes, F.; Ludwig, W.; Schauermann, S.; Neyman, K. M. Tuning the Surface Chemistry of Pd by Atomic C and H: A Microscopic Picture. *Chem. - Eur. J.* **2013**, *19* (4), 1335−1345.
(25) Bertolini, J. C.; Rousset, J. L. Reactivity of Metal Nanoparticles. In *Nanomaterials and Nanochemistry*; Bréchignac, C., Houdy, P., L, M., Eds.; Springer-Verlag: Berlin, 2008; pp 281−304.
(26) Zaera, F. Nanostructured Materials for Applications in Heterogeneous Catalysis. *Chem. Soc. Rev.* **2013**, *42* (7), 2746−2762.
(27) Zaera, F. Shape-Controlled Nanostructures in Heterogeneous Catalysis. *ChemSusChem* **2013**, *6* (10), 1797−1820.
(28) Zaera, F. New Challenges in Heterogeneous Catalysis for the 21st Century. *Catal. Lett.* **2012**, *142*, 501−516.
(29) Schauermann, S.; Nilius, N.; Shaikhutdinov, S.; Freund, H.-J. Nanoparticles for Heterogeneous Catalysis: New Mechanistic Insights. *Acc. Chem. Res.* **2013**, *46* (8), 1673−1681.
(30) Freund, H.-J.; Nilius, N.; Risse, T.; Schauermann, S. A Fresh Look at an Old Nano-Technology: Catalysis. *Phys. Chem. Chem. Phys.* **2014**, *16* (18), 8148−8167.
(31) Schauermann, S.; Freund, H.-J. Model Approach in Heterogeneous Catalysis: Kinetics and Thermodynamics of Surface Reactions. *Acc. Chem. Res.* **2015**, *48* (10), 2775−2782.
(32) Neyman, K. M.; Schauermann, S. Hydrogen Diffusion into Palladium Nanoparticles: Pivotal Promotion by Carbon. *Angew. Chem., Int. Ed.* **2010**, *49* (28), 4743−4746.
(33) Aleksandrov, H. A.; Kozlov, S. M.; Schauermann, S.; Vayssilov, G. N.; Neyman, K. M. How Absorbed Hydrogen Affects the Catalytic Activity of Transition Metals. *Angew. Chem., Int. Ed.* **2014**, *53* (49), 13371−13375.
(34) Si, Y.; Samulski, E. T. Exfoliated Graphene Separated by Platinum Nanoparticles. *Chem. Mater.* **2008**, *20* (21), 6792−6797.
(35) Hsieh, S. H.; Hsu, M. C.; Liu, W. L.; Chen, W. J. Study of Pt Catalyst on Graphene and Its Application to Fuel Cell. *Appl. Surf. Sci.* **2013**, *277*, 223−230.
(36) Marinkas, A.; Arena, F.; Mitzel, J.; Prinz, G. M.; Heinzel, A.; Peinecke, V.; Natter, H. Graphene as Catalyst Support: The Influences of Carbon Additives and Catalyst Preparation Methods on the Performance of PEM Fuel Cells. *Carbon* **2013**, *58* (i), 139−150.
(37) Lazzarini, A.; Piovano, A.; Pellegrini, R.; Leofanti, G.; Agostini, G.; Rudić, S.; Chierotti, M. R.; Gobetto, R.; Battiato, A.; Spoto, G.; et al. A Comprehensive Approach to Investigate the Structural and Surface Properties of Activated Carbons and Related Pd-Based Catalysts. *Catal. Sci. Technol.* **2016**, *6* (13), 4910−4922.
(38) Maiyalagan, T.; Wang, X.; Manthiram, A. Highly Active Pd and Pd-Au Nanoparticles Supported on Functionalized Graphene Nanoplatelets for Enhanced Formic Acid Oxidation. *RSC Adv.* **2014**, *4* (8), 4028−4033.
(39) Wei, Z.; Pan, R.; Hou, Y.; Yang, Y.; Liu, Y. Graphene-Supported Pd Catalyst for Highly Selective Hydrogenation of Resorcinol to 1, 3-Cyclohexanedione through Giant π-Conjugate Interactions. *Sci. Rep.* **2015**, *5* (1), 15664.
(40) Ströbel, R.; Garche, J.; Moseley, P. T.; Jörissen, L.; Wolf, G. Hydrogen Storage by Carbon Materials. *J. Power Sources* **2006**, *159* (2), 781−801.
(41) Zhou, C.; Szpunar, J. A. Hydrogen Storage Performance in Pd/Graphene Nanocomposites. *ACS Appl. Mater. Interfaces* **2016**, *8* (39), 25933−25940.
(42) Vinayan, B. P.; Sethupathi, K.; Ramaprabhu, S. Investigations of Hydrogen Storage in Palladium Decorated Graphene Nanoplatelets. *Trans. Indian Inst. Met.* **2011**, *64* (1−2), 169−173.
(43) Rupprechter, G.; Morkel, M.; Freund, H.-J.; Hirschl, R. Sum Frequency Generation and Density Functional Studies of CO-H Interaction and Hydrogen Bulk Dissolution on Pd(111). *Surf. Sci.* **2004**, *554* (1), 43−59.
(44) Doyle, A. M.; Shaikhutdinov, S. K.; Freund, H.-J. Surface-Bonded Precursor Determines Particle Size Effects for Alkene Hydrogenation on Palladium. *Angew. Chem., Int. Ed.* **2005**, *44* (4), 629.
(45) Nikolaev, S. A.; Zanaveskin, L. N.; Smirnov, V. V.; Averyanov, V. A.; Zanaveskin, K. L. Catalytic Hydrogenation of Alkyne and Alkadiene Impurities from Alkenes. Practical and Theoretical Aspects. *Russ. Chem. Rev.* **2009**, *78* (3), 231−247.
(46) Hu, B.; Deng, W.; Li, R.; Zhang, Q.; Wang, Y.; Delplanque-Janssens, F.; Paul, D.; Desmedt, F.; Miquel, P. Carbon-Supported Palladium Catalysts for the Direct Synthesis of Hydrogen Peroxide from Hydrogen and Oxygen. *J. Catal.* **2014**, *319*, 15−26.
(47) Semikolenov, V. A. Modern Approaches to the Preparation of "Palladium on Charcoal" Catalysts. *Russ. Chem. Rev.* **1992**, *61*, 168.
(48) Canton, P.; Fagherazzi, G.; Battagliarin, M.; Menegazzo, F.; Pinna, F.; Pernicone, N. Pd /CO Average Chemisorption Stoichiometry in Highly Dispersed Supported Pd/γ-Al_2O_3. *Langmuir* **2002**, *18* (17), 6530−6535.
(49) Ohshima, H. Zeta Potential. In *Encyclopedia of Colloid and Interface Science*; Springer: Berlin, 2013; pp 148−207.
(50) Clogston, J. D. Measuring Zeta Potential of Nanoparticles. *NCL Method PCC-2* **2009**, *21702* (Nov), 14.
(51) Zuccaro, L.; Krieg, J.; Desideri, A.; Kern, K.; Balasubramanian, K. SI:Tuning the Isoelectric Point of Graphene by Electrochemical Functionalization. *Sci. Rep.* **2015**, *5*, 11794.
(52) Bugaev, A. L.; Usoltsev, O. A.; Lazzarini, A.; Lomachenko, K. A.; Guda, A. A.; Pellegrini, R.; Carosso, M.; Vitillo, J. G.; Groppo, E.; van Bokhoven, J. A.; Soldatov, A. V.; Lamberti, C. Time-Resolved Operando Studies of Carbon Supported Pd Nanoparticles under Hydrogenation Reactions by X-Ray Diffraction and Absorption. *Faraday Discuss.* **2018**, *208*, 187.
(53) Bugaev, A. L.; Guda, A. A.; Lomachenko, K. A.; Bugaev, L. A.; Soldatov, A. V. Pd Hydride and Carbide Studied by Means of Pd K-Edge X-Ray Absorption near-Edge Structure Analysis. *Bull. Russ. Acad. Sci.: Phys.* **2015**, *79* (9), 1180−1185.
(54) Raymundo-Pinero, E.; Azais, P.; Cacciaguerra, T.; Cazorla-Amoros, D.; Linares-Solano, A.; Beguin, F. KOH and NaOH Activation Mechanisms of Multiwalled Carbon Nanotubes with Different Structural Organisation. *Carbon* **2005**, *43* (4), 786−795.
(55) Lööf, P.; Stenbom, B.; Nordén, H.; Kasemo, B. Rapid Sintering in NO of Nanometer-Sized Pt Particles on γ-Al_2O_3 Observed by CO Temperature-Programmed Desorption and Transmission Electron Microscopy. *J. Catal.* **1993**, *144* (1), 60−76.
(56) Föttinger, K.; Schlögl, R.; Rupprechter, G. The Mechanism of Carbonate Formation on Pd-Al_2O_3 Catalysts. *Chem. Commun.* **2008**, *3* (3), 320−322.
(57) Primo, A.; Neatu, F.; Florea, M.; Parvulescu, V.; Garcia, H. Graphenes in the Absence of Metals as Carbocatalysts for Selective Acetylene Hydrogenation and Alkene Hydrogenation. *Nat. Commun.* **2014**, *5*, 5291.
(58) Rupprechter, G.; Unterhalt, H.; Morkel, M.; Galletto, P.; Hu, L.; Freund, H.-J. Sum Frequency Generation Vibrational Spectroscopy at Solid-Gas Interfaces: CO Adsorption on Pd Model Catalysts at Ambient Pressure. *Surf. Sci.* **2002**, *502*−*503*, 109−122.
(59) Molero, H.; Stacchiola, D.; Tysoe, W. T. The Kinetics of Ethylene Hydrogenation Catalyzed by Metallic Palladium. *Catal. Lett.* **2005**, *101* (3−4), 145−149.

https://dx.doi.org/10.1021/acs.jpcc.0c06636
J. Phys. Chem. C 2020, 124, 23674−23682

(60) Stacchiola, D.; Calaza, F.; Zheng, T.; Tysoe, W. T. Hydrocarbon Conversion on Palladium Catalysts. *J. Mol. Catal. A: Chem.* **2005**, *228* (1−2), 35−45.
(61) Beebe, T. P.; Yates, J. T. An in Situ Infrared Spectroscopic Investigation of the Role of Ethylidyne in the Ethylene Hydrogenation Reaction on Pd/Al_2O_3. *J. Am. Chem. Soc.* **1986**, *108* (4), 663−671.
(62) Rupprechter, G.; Somorjai, G. A. Palladium-Catalyzed Hydrogenation without Hydrogen: The Hydrodechlorination of Chlorofluorocarbons with Solid State Hydrogen over the Palladium (111) Crystal Surface and Its Implications. *Catal. Lett.* **1997**, *48*, 17−20.
(63) Deerattrakul, V.; Yigit, N.; Rupprechter, G.; Kongkachuichay, P. The Roles of Nitrogen Species on Graphene Aerogel Supported Cu-Zn as Efficient Catalysts for CO_2 Hydrogenation to Methanol. *Appl. Catal., A* **2019**, *580*, 46−52.
(64) Möbus, K.; Grünewald, E.; Wieland, S. D.; Parker, S. F.; Albers, P. W. Palladium-Catalyzed Selective Hydrogenation of Nitroarenes: Influence of Platinum and Iron on Activity, Particle Morphology and Formation of β-Palladium Hydride. *J. Catal.* **2014**, *311*, 153−160.
(65) Parker, S. F.; Walker, H. C.; Callear, S. K.; Grünewald, E.; Petzold, T.; Wolf, D.; Möbus, K.; Adam, J.; Wieland, S. D.; Jiménez-Ruiz, M.; et al. The Effect of Particle Size, Morphology and Support on the Formation of Palladium Hydride in Commercial Catalysts. *Chem. Sci.* **2019**, *10* (2), 480−489.
(66) Chesters, M. A.; Packer, K. J.; Viner, H. E.; Wright, M. A. P.; Lennon, D. 1H NMR of Hydrogen Chemisorbed on Silica-Supported Platinum Particles: An Evaluation of Different Models. *J. Chem. Soc., Faraday Trans.* **1995**, *91* (14), 2203−2206.
(67) Chesters, M. A.; Packer, K. J.; Viner, H. E.; Wright, M. A. P.; Lennon, D. Variable-Temperature, 1H NMR Study of Hydrogen Chemisorption on EuroPt-1. *J. Chem. Soc., Faraday Trans.* **1996**, *92* (23), 4709−4716.

https://dx.doi.org/10.1021/acs.jpcc.0c06636
J. Phys. Chem. C 2020, 124, 23674−23682